

Crystallization of Compound Plastic Optical Fibers

J.I. Ramos ^a, Francisco J. Blanco-Rodríguez ^{b, *}

^a Universidad de Málaga, Escuela de Ingenierías, Room 2.139.D, c/ Doctor Ortiz Ramos s/n, 29071, Málaga, Spain.

^b Universidad de Málaga, Escuela de Ingenierías, Room 2.140.D, c/ Doctor Ortiz Ramos s/n, 29071, Málaga, Spain.

Abstract

A mathematical model of the spinning of compound, plastic optical fibers which accounts for molecular orientation and crystallization is presented. The model employs a Newtonian rheology, includes the effects of both temperature and flow-induced crystallization, and accounts for the effects of the molecular orientation on the stress tensor through a Doi-Edwards formulation. For slender fibers, an asymptotic procedure based on the slenderness ratio shows that the temperature is uniform across the compound fiber provided that the Biot number is on the order of the fourth power of the slenderness ratio and the leading-order equations for the fiber's geometry and axial velocity component, temperature, molecular orientation and crystallization are one-dimensional. A two-dimensional model based on the leading-order equations for the fiber's geometry and velocity for slender fibers is also presented; this model provides the two-dimensional fields of temperature, molecular orientation and degree of crystallization and indicates that, for moderate Biot numbers, the temperature distribution across the fiber is not uniform and a thermal boundary layer is formed on the outer surface of the compound fiber.

Keywords: Plastic optical fibers; compound fibers; orientation; crystallization.

Nomenclature

a_2	Constant of the linearized crystal growth rate
A	Pre-exponential factor, N s/m ²
c	Number of polymeric units per unit volume, 1/m ³
C	Specific heat, J/kg K
D	Pre-exponential factor (linear approximation), N s/m ²
E	Activation temperature, K
f^m	Body force per unit mass, N/kg
g	Gravitational acceleration, 9.81 m/s ²
h	Film heat transfer coefficient, W/K m ²
H	Activation temperature, 1/K
k	Thermal conductivity, W/m K
k_A	Linearized crystal growth rate
$k_A(0)$	Amorphous growth rate
k_B	Boltzmann constant, 1.38065·10 ⁻²³ m ² kg/s ² K
L	Characteristic length in the axial direction, m
n	Crystallization viscosity index
N	Dimensionless measure of c
p	Pressure, N/m ²
r	Radial coordinate, m
R	Radius of the jet, m
\tilde{R}	Non-dimensional radius of the fiber
S	Molecular orientation order parameter
t	Time, s
T	Temperature of the jet, K
\hat{T}	Non-dimensional temperature of the fiber
\mathbf{T}	Stress tensor, N/m ²

\hat{U}	Non-dimensional axial velocity
\mathbf{v}	Velocity vector, m/s
\hat{V}	Non-dimensional radial velocity
x	Axial coordinate, m

Greek Symbols

α	Relation between kinetic and internal energies
β	Crystallization viscosity rate
ϵ	Slenderness ratio
η	Map of the non-dimensional axial coordinate
θ	Degree of crystallinity
λ	Relaxation time, s
μ	Dynamic viscosity, Pa s
ξ	Map of the non-dimensional radial coordinate
ρ	Mass density, kg/m ³
σ	Surface tension, N/m
ϕ	Dimensionless parameter related to the friction tensor

Subscripts

0	Reference value
1	Inner jet
2	Outer jet
∞	Surrounding medium
m	Melting
eff	Effective

Non-dimensional numbers

Re	Reynolds number, $[\rho_0 u_0 R_0 / \mu_0]$
------	---

* Corresponding author. Tel.: +34 951952522
Fax: +34 952131397; E-mail: fjblanco@lcc.uma.es

Pe	Péclet number, $[\rho_0 u_0 R_0 C_0 / k_0]$
Ca	Capillarity number, $[\mu_0 u_0 / \sigma_2]$
Fr	Froude number, $\left[\frac{u_0^2}{g R_0} \right]$
Bi	Biot number, $[h R_0 / k_2]$

1. Introduction

Many optical, textile, electrically conducting, and reinforced fibers are manufactured by melt-spinning processes [1, 2, 3, 4]. There are mainly two methods for the fabrication of high-bandwidth, low attenuation graded-index plastic optical fibers (POF). The first one is usually referred to as the preform technique and is based on interfacial gel polymerization, but it is too expensive to be adopted for mass production. The second process of graded-index (GI) POF manufacturing is called co-extrusion. In this process, monomers doped with low-molecular weight molecules and homogeneous monomers are polymerized as core and cladding or sheath polymers, respectively. The two materials are then melted in their respective parts and compounded in a die to fabricate a POF that has a concentric circular core/cladding structure which does not exhibit at this stage a graded refractive index distribution. By heating the fiber in a diffusion section, a radial concentration profile of low-weight molecules is formed as a result of molecular diffusion. Solidification takes place between the plate and a rotating drum, and large extensions rates, rapid cooling, and high speeds are usually involved. Finally, the GI POF is obtained by winding it on a take-up reel.

In some compound fibers, the cladding material either protects the core, serves as a waveguide in signal transmission or is a more costly material than the core with more desirable surface properties. It must be noted that, in general, the combination of two different materials with different properties can result in a composite fiber with desirable global properties.

The properties of plastic products manufactured by heating the polymer to above its melting temperature and then deforming the melt while simultaneously cooling it, depend on the processing conditions to which the polymer is subject during its manufacture. Depending on the molecular structure and processing conditions, the final product can be in either an amorphous or a semi-crystalline state. Polymers that are unable to crystallize on cooling below their glass transition temperature, form amorphous solids, and, if these solids are formed by deforming the polymer while cooling it through the glass transition temperature, they can exhibit strong anisotropy.

Previous studies of bi-component fibers have been mainly concerned with one-dimensional models of amorphous, slender fibers at low Reynolds numbers based on either simplified models or an asymptotic analysis of the full governing equations that uses the

slenderness ratio as the small perturbation parameter. In addition, these studies have been mainly concerned with isothermal flows [5, 6, 7, 8, 9]. Non-isothermal studies of bi-component fibers include that of Kikutani et al. [10] who modelled the high-speed melt spinning of bi-component fibers consisting of poly(ethylene terephthalate) (PET) in the core and polypropylene (PP) in the cladding by means of simple, one-dimensional equations of mass, linear momentum and energy conservation, and included both Newtonian and upper-convected Maxwell rheologies and drag on the fiber.

A one-dimensional model of semi-crystalline, bi-component fibers that accounts for molecular orientation and crystallization but does not include the latent heat of crystallization was developed by one of the authors [11]. Such a model is governed by one-dimensional partial differential equations for the leading-order geometry, axial velocity component and temperature that were derived from the conservation equations of mass, linear momentum and energy under the assumptions that the fiber is slender and the Reynolds and Biot numbers are small. The effects of the molecular orientation and crystallization were added to this model by considering two transport equations for these two quantities. The molecular orientation model was based on Doi's slender body theory of liquid crystalline polymers, while the crystallization kinetics used Avrami-Kolmogorov's theory [12, 13] with Ziabicki's model [14] for the coupling between the crystallinity and the polymer orientation, and Kikutani's empirical law [15, 16] was employed to relate the elongational viscosity of the melt to the degree of crystallinity.

In this paper, we present a two-dimensional model of semi-crystalline bi-component fiber spinning processes that uses a modified Newtonian rheology, accounts for the degrees of molecular orientation and crystallization, and allows to determine the radial variations of these quantities across the fiber.

2. Mathematical model of melt spinning

We consider an axisymmetric, bi-component or compound liquid jet such as the one shown schematically in Fig. 1, consisting of two immiscible, incompressible (constant density) fluids which are assumed to be Newtonian. The inner (subscript 1) and outer (subscript 2) jets correspond to $0 < r < R_1(t, x) \equiv R(t, x)$ and $R_1(t, x) < r < R_2(t, x)$, respectively, where $r = R_1$ and $r = R_2$ denote the core and the cladding outer radii, respectively.

The fluid dynamics of bi-component fibers are governed by the two-dimensional conservation equations of mass (1), linear momentum (2) and energy (3),

$$\nabla \cdot \mathbf{v}_i = 0 \quad (1)$$

$$\rho_i \left(\frac{\partial \mathbf{v}_i}{\partial t} + \mathbf{v}_i \cdot \nabla \mathbf{v}_i \right) = -\nabla p_i + \nabla \cdot \mathbf{T}_i + \rho_i \mathbf{f}^m \quad (2)$$

$$\rho_i C_i \left(\frac{\partial T_i}{\partial t} + \mathbf{v}_i \cdot \nabla T_i \right) = k_i \Delta T_i \quad (3)$$

where $\mathbf{v} = u(r, x)\hat{\mathbf{e}}_x + v(r, x)\hat{\mathbf{e}}_r$ and $\mathbf{f}^m = g\hat{\mathbf{e}}_x$.

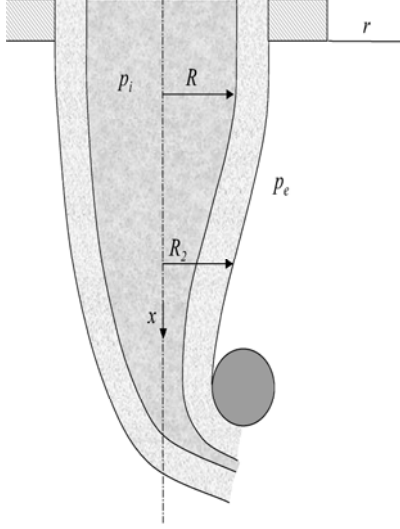


Fig. 1. Schematic of a compound fiber.

In the model presented here, we shall assume that the density, specific heat, thermal conductivity, and surface tension, are assumed to be constant, and the gases surrounding the outer jet are dynamically passive. The latter assumption can be justified due to the small density and dynamic viscosity of gases compared with those of liquids. In addition, it is assumed that the dynamic viscosity, μ , of the two components of the fiber depends in an Arrhenius fashion on the temperature, T , and can be written as

$$\mu_i = A_i \exp\left(-\frac{E_i}{T_i - (T_m)_i}\right) \quad i = 1, 2, \quad (4)$$

where E and T_m denote the activation temperature, i.e., the activation energy divided by the universal gas constant, and melting temperature, respectively.

This equation can be linearized and written as

$$\mu_i = D_i \exp(H_i ((T_m)_i - T_i)) \quad i = 1, 2, \quad (5)$$

which indicates that the dynamic viscosity increases exponentially with the temperature for $T < T_m$, and the values of D and H can be easily deduced from Eq. (4).

The degree of orientation for the order parameter, $S(r, x)$, has been modelled as an ensemble average of the alignment of the molecular direction with respect to the axial direction and is determined by the following equation

$$\frac{\partial S}{\partial t} + \mathbf{v} \cdot \nabla S = -\frac{\phi}{\lambda} U(S) + G(\nabla \mathbf{v}, S), \quad (6)$$

where,

$$U(S) = S \left(1 - \frac{N}{3}(1 - S)(2S + 1)\right), \quad (7)$$

is a bulk free energy which is related to the intermolecular potential, ϕ is an anisotropic drag parameter ($0 \leq \phi \leq 1$, $\phi = 1$ for isotropic models, and $\phi \approx 0.5$ for rigid-rod molecular models), λ is the molecular relaxation time of the liquid-crystalline polymer, N is the dimensionless density of the liquid-crystalline polymer and is directly proportional to the excluded volume between two rigid rods where each rod represents a polymer molecule and

$$G(\nabla \mathbf{v}, S) = (1 - S)(2S + 1) \frac{\partial u}{\partial x}. \quad (8)$$

In order to account for the effects of both amorphous and crystalline phases, we have assumed that the semi-crystalline materials that compose the core and cladding behave as single-phase fluids where the degree of crystallization ($\theta(r, x)$) has been modelled by means of Ziabicki's model [14]

$$\frac{\partial \theta_i}{\partial t} + \mathbf{v}_i \cdot \nabla \theta_i = k_{Ai}(S)(\theta - \theta_{\infty,i}) \quad i = 1, 2, \quad (9)$$

where

$$k_{Ai}(S) = k_{Ai}(0) \exp(a_{2i} S_i^2) \quad i = 1, 2, \quad (10)$$

is the linearized crystal growth rate, $k_{Ai}(0)$ is the amorphous growth rate. The molecular orientation and crystallization of compound fibers requires the solution of this set of partial differential equations where μ_i is to be replaced by an effective dynamic viscosity, $\mu_{eff,i}$, given by

$$\mu_{eff,i} = \mu(T_i) \exp\left(\beta_i \left(\frac{\theta}{\theta_{\infty,i}}\right)^{n_i}\right) + \frac{2}{3} \alpha_i \lambda_i S_i^2, \quad (11)$$

$i = 1, 2$, where α is a parameter that relates the kinetic energy to the inertial energy of the liquid-crystalline polymer, β and n are material-dependent, e.g., $\beta = 4.605$ and $n = 12$ for nylon-66, $\beta = 4.0$ and $n = 2$ for PET, and the effects of crystallization on the effective dynamic viscosity have been assumed to be multiplicative, whereas those of the molecular orientation have been assumed to be additive. Equation (11) indicates that the molecular orientation and the degree of crystallization affect the effective viscosity and, therefore, the contribution of the Newtonian stress tensor.

Equation (6) indicates that the molecular orientation parameter is affected velocity and the velocity gradient and affects the degree of crystallization through Eq. (9); both the orientation and crystallization affect the velocity (Eq. (2)) through the effective dynamic viscosities (Eq. (11)), and, of course, the compound fiber's geometry and temperature (Eq. (3)) are affected by the velocity field. This implies that the orientation and crystallization of the compound fiber are nonlinearly coupled with the fiber's geometry, axial velocity component and temperature. Therefore, Eqs. (1)-(3), (6) and (9) must be solved numerically in an iterative fashion subject to specified conditions at the die exit $x = 0$, downstream or take-up location $x = L$, initial conditions and symmetry boundary conditions at the centerline $r = 0$. In addition, at the to-be-determined core-cladding, $r = R_1$, and cladding-surroundings, $r = R_2$, interfaces which are assumed to be material surfaces, kinematic and dynamic boundary conditions that specify the continuity of radial and axial velocity components and tangential stresses, and the difference between normal stresses is balanced by surface tension, must be applied. Moreover, at $r = R_1$, there is continuity of temperatures and heat flux, while, at $r = R_2$, the heat flux from conduction in the cladding was assumed equal to $h(T(t, R_2, x) - T_\infty)$ where T_∞ is the temperature of the gases that surround the fiber, and the film heat transfer coefficient h could depend on the local Reynolds and Prandtl numbers [17].

3. Numerical method

For steady-state slender fibers, $\epsilon = \frac{R_0}{L} \ll 1$, it is convenient to non-dimensionalize the variables $r, x, u, v, p, T, \rho, C, \mu$ and k with respect $R_0, L, u_0, v_0 = \epsilon u_0, p_0 = \frac{\mu_0 u_0}{L}, T_0, \rho_0, C_0, \mu_0$ and k_0 respectively, where R_0 is the die exit radius, L is the distance between the die exit and the take-up point and T_0 is the largest melting temperature of the core and cladding. With this non-dimensionalization, it can be easily shown by means of perturbation methods based on the slenderness ratio that, for slender fibers, the leading-order non-dimensional axial velocity component is only a function of \hat{x} ($\hat{u}_i(\hat{r}, \hat{x}) = \hat{U}(\hat{x})$), and the leading-order non-dimensional radial velocity component (cf. Eq. (1)) is given by

$$\hat{v}(\hat{r}, \hat{x}) = \hat{V}(\hat{r}, \hat{x}) = -\frac{\hat{r}}{2} \frac{d\hat{U}}{d\hat{x}}. \quad (12)$$

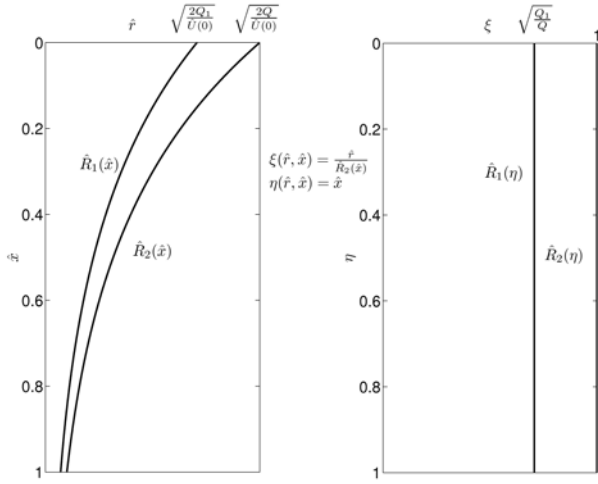


Fig. 2. Transformation map.

The dimensionless parameters governing the problem are the Reynolds, Froude, capillarity, Péclet and Biot numbers.

The dimensionless volumetric flow rates for the core and cladding are given by the kinematics conditions at the interfaces and can be written as

$$Q_1 = \frac{\hat{R}_1^2(\hat{x})}{2} \hat{U}(\hat{x}), \quad Q_2 = \frac{\hat{R}_2^2(\hat{x}) - \hat{R}_1^2(\hat{x})}{2} \hat{U}(\hat{x}). \quad (13)$$

The numerical solution of the equations governing the two-dimensional free-surface model for compound plastic fibers presented in the last section was obtained using the transformation $(\hat{r}, \hat{x}) \rightarrow (\xi, \eta)$ for the inner and outer jets, where $\eta = \hat{x}$ and $\xi = \frac{\hat{r}}{R_2(\hat{x})}$ that maps the curvilinear geometries of the inner and outer fibers into rectangles, i.e., $[0, R_1(\hat{x})] \rightarrow [0, \sqrt{\frac{Q_1}{Q}}]$ and $[R_1(\hat{x}), R_2(\hat{x})] \rightarrow [\sqrt{\frac{Q_1}{Q}}, 1]$, respectively, where $Q = Q_1 + Q_2$ denotes the non-dimensional volumetric flow rate of the compound fiber. Under these conditions, the axial momentum equation is one-dimensional and of the advection-diffusion type, whereas Eq. (13) provides $\hat{R}_1(\hat{x})$ and $\hat{R}_2(\hat{x})$. The equation for the molecular orientation parameter and the degree of crystallization are hyperbolic

and can be easily solved by means of an implicit method, whereas the (two-dimensional) energy equation is of the advection-diffusion type and was solved by sweeping on the axial direction and iterating in the radial one on grids consisting of 1001 and 501 (201 for the core and 301 for the cladding, respectively) points in the axial and radial directions, respectively, until the L_2 norm of the differences between the solutions in two successive iterations was less than or equal to 10^{-8} .

4. Simulation results of melt spinning fibers

In this section, we illustrate some sample two-dimensional results of the axisymmetric melt spinning model for semi-crystalline compound fiber described above.

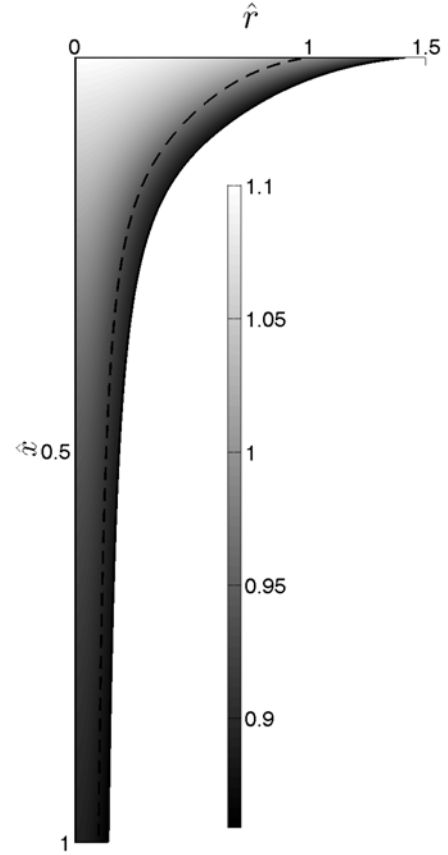


Fig. 3. Non-dimensional temperature field of a compound fiber ($Bi = 0.5$).

In the results presented below, we have used the same thermal conductivities and pre-exponential factors of the dynamic viscosity for the core and cladding, a constant film-heat transfer coefficient that corresponds to a Biot number equal to 0.5 and 5 and unity Reynolds, Froude and Péclet numbers. Imposing $\hat{R}_1(0) = 1$ and $Q_1 = 0.5$ (we have used the same non-dimensional volumetric flow for the core and the cladding, $Q_1 = Q_2$) implies (cf. Eq. 13) that the non-dimensional axial velocity at the die exit is unity. In the cases considered here, the draw ratio, D_r , the relation between the axial velocity at the take-up location and that at the nozzle exit is 100. The relevant processing parameters are summarized in Table 1.

Table 1. Simulation parameters.

Case	H_1	H_2	Bi	Pe	D_1/D_2	λ_i	ϕ_i	Ca
1	20	10	0.5	1	1	1	0.5	10
2	20	10	5.0	1	1	1	0.5	10

The others parameters of the problem have been selected as $N_i = 4$, $\alpha_i = 5$, $a_{21} = 10$, $a_{22} = 5$, $n_i = 12$, $\beta_i = 4$, $\sigma_1/\sigma_2 = \rho_1/\rho_2 = C_1/C_2 = 1$, $\beta_i = 4$, $k_{A1}(0) = k_{A1}(0) = 0.005$, $T_\infty = p_\infty = 0$ and $\theta_{\infty,i} = 0.8$.

In Figures 3 and 4, we show some sample results that illustrate the non-dimensional temperature field in the compound fiber as a function of the non-dimensional axial and radial coordinates.

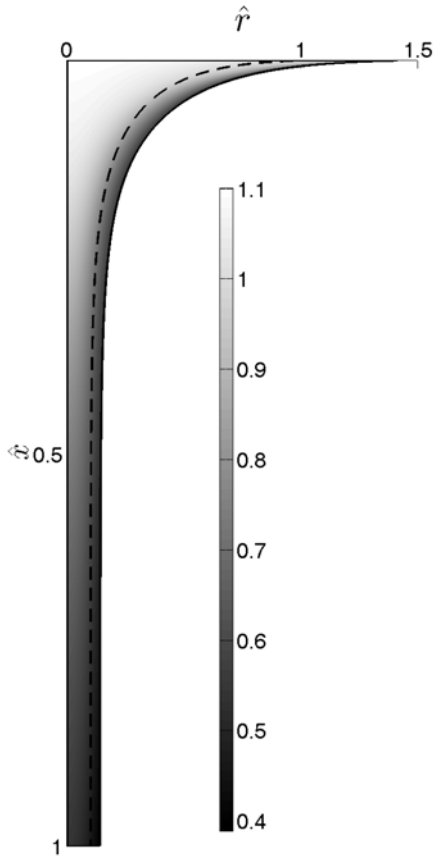


Fig. 4. Non-dimensional temperature field of a compound fiber ($Bi = 5$).

Figure 3 corresponds to an average Biot number of 0.5 and clearly indicates that a thermal boundary layer forms at R_2 and that the temperature of the core is initially almost uniform in the radial direction.

Figure 4 corresponds to an average Biot number ten times larger than that of Fig. 3 and shows that, as the Biot number increases, the heat transfer by conduction from the cladding to the surroundings increases, thereby increasing the heat flux at R_1 and decreasing the temperature of the core. In this case a small temperature gradient in the radial direction can be observed at $\hat{x} = 1$.

Figure 5 illustrates the numerical results obtained for the leading order geometry and axial velocity component and the average temperature, effective dynamic viscosity and molecular orientation parameter and degree of crystallinity of the compound fiber for the conditions of

Table 1. This figure shows that the compound fiber undergoes a drastic change in geometry near the die exit and its two radii become constant once the effective viscosity becomes very large. The effective viscosity increases as the temperature decreases in accord with the Arrhenius expression used in this study.

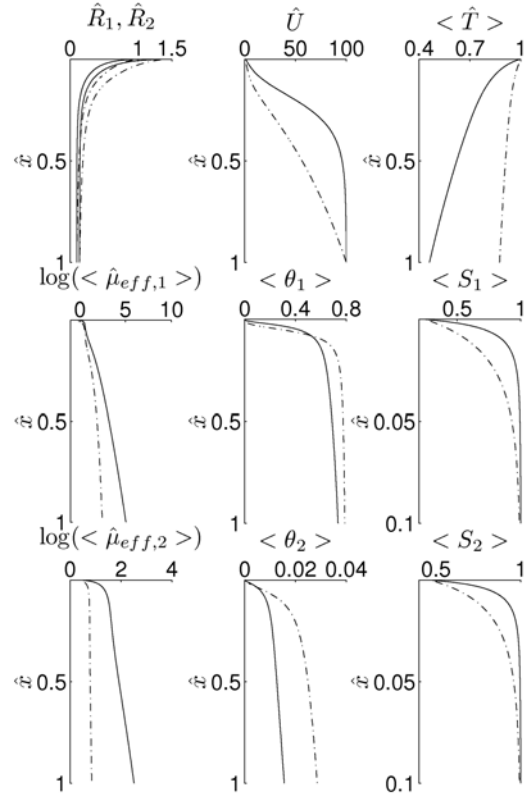


Fig. 5. (From left to right) First row: Compound fiber geometry, axial velocity component, and average of temperature. Second row and third row: (decimal logarithm of) effective dynamic viscosity, degree of crystallization and molecular orientation parameter for the core and cladding for cases 1 (— · —) and 2 (—) of Table 1.

Figure 5 also shows that the fiber's axial velocity increases very rapidly near the die exit and reaches a constant value once the dynamic viscosity becomes very large. On the other hand, the fiber's cross-sectionally averaged temperature decreases slowly, the molecular orientation increases rapidly towards its final value of unity, i.e., complete orientation is achieved, while the degree of crystallization is very sensitive to the values of the constants that appear in its evolution equation.

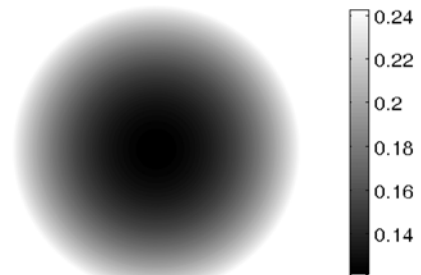


Fig. 6. Degree of crystallization of the core at $\hat{x} = 0.04$.

Figure 5 also indicates that the rate of crystallization is positive at the take-up point in accord with the negative temperature gradient there.

Figures 6 and 7 show the degree of crystallization in the core at $\hat{x} = 0.04$ and $\hat{x} = 0.1$, respectively, for the core. These two figures clearly indicate that crystallization in the compound fiber for the conditions analyzed here is mainly a thermal process and that the flow-induced crystallization is small. Although not shown here, the degree of crystallization increases first rather quickly and then levels off. This behaviour is more clearly illustrated in the averaged crystallinity profiles illustrated in Fig. 5.

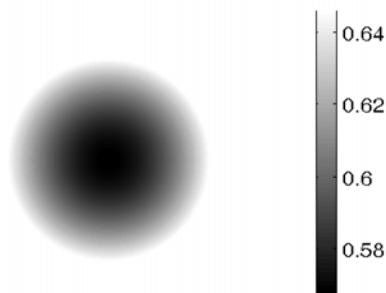


Fig. 7. Degree of crystallization of the core at $\hat{x} = 0.1$.

5. Discussion

A single-phase two-dimensional model of the spinning of compound plastic optical fibers that employs a Newtonian rheology modified by the degrees of crystallization and molecular orientation and accounts for temperature through an effective dynamic viscosity, and the molecular orientation of the liquid crystalline polymer through an orientation parameter that depends on the velocity field, has been proposed. For slender fibers and very low Biot numbers, an asymptotic analysis of the model yields one-dimensional equations for the leading-order axial velocity, temperature, orientation parameter and degree of crystallization provided that the molecular orientation tensor is diagonal. For higher Biot numbers, radial variations of temperature across the fiber are important and, consequently, a two-dimensional model was developed and solved numerically. Its results indicate that substantial temperature non-uniformities in the radial direction exist even at small Biot numbers. These non-uniformities affect the degree of crystallization and have great effects on the mechanical, electrical, optical, etc., properties of compound fibers. For very slender fibers and small Biot numbers, good agreement between the leading-order one-dimensional model for slender fibers and the two-dimensional one presented here has been observed. In addition, It was found that the crystallization of the compound fiber was mostly affected by thermal effects rather than by flow-induced ones.

Acknowledgments

The research reported in this paper was supported by Project FIS2009-12894 and FPU grant reference number AP2006-02242 from the Ministerio de Ciencia e Innovación of Spain.

References

- [1] Shah Khan, MZ, Simpson, G, Gellert, EP. Resistance of Glass-fiber Reinforced Polymer Composites to Increasing Compressive Strain Rates and Loading Rates, *Composites: Part A* 2000; 31:57-67.
- [2] Huang, J, Baird, DG, Loos, AC, Rangarajan, P, Powell, A. Filament Winding of Bicomponent Fibers Consisting of Polypropylene and a Liquid Crystalline Polymer, *Composites: Part A* 2001; 32:1013-1020.
- [3] Zubia, J. and Arrue, J. *Plastic Optical Fibers: An Introduction to Their Technological Processes*, *Optical Fiber Technology* 2001, 7:101-140.
- [4] Koike, Y, Asai, M. The Future of Plastic Optical Fiber, *NPG Asia Materials* 2009, 1:22-28.
- [5] Lee, WS, Park, CW. Stability of a Bicomponent Fiber Flow, *ASME Journal of Applied Mechanics* 1995, 62:511-516.
- [6] Ji, CC, Yang, JC. *Mechanics of Steady Flow in Co-extrusion Fiber Spinning*, *Polymer Engineering Science* 1996, 36:1399-1409.
- [7] Naboulsi, SK, Bechtel, SE. *Bicomponent Newtonian Fibers*, *Physics of Fluids* 1999, 11:807-820.
- [8] Ramos, JI. *Asymptotic Analysis of Compound Liquid Jets at Low Reynolds Numbers*, *Applied Mathematics and Computation*. 1999, 100:223-240.
- [9] Ramos, JI. *Compound Liquid Jets at Low Reynolds Numbers*, *Polymer* 2002, 43:2889-2896.
- [10] Kikutani, K, Radhakrishnan, J, Arikawa, S, Takaku, A, Okui, N, Jin, X, Niwa, F, Kudo, Y. High-speed Melt Spinning of Bicomponent Fibers: Mechanism of Fiber Structure Development in Poly(ethylene terephthalate)/Polypropylene System, *Journal of Applied Polymer Science* 1996, 62:1913-1924.
- [11] Ramos, JI. *Modelling of Liquid Crystalline Compound Fibers*, *Polymer* 2005, 46:12612-12625.
- [12] Avrami, M. Kinetics of Phase Change. III. Granulation, Phase Change, and Microstructure, *Journal Chemical Physics* 1941, 9:177-184.
- [13] Kolmogorov, AN. On the Statistical Theory of the Crystallization of Metals, *Bulletin of the Academy of Sciences of the USSR, Mathematical Series* 1937, 1:355-359.
- [14] Ziabicki, A. *Fundamentals of Fiber Formation*, eds. John Wiley & Sons, New York, USA, 1976.
- [15] Ziabicki, A, Kawai, H, *High Speed Fiber Spinning*, eds. John Wiley & Sons, New York, USA, 1985.
- [16] Ziabicki, A, Jarecki, A, Wasiak, A. *Dynamic Modelling of Melt Spinning*, *Computational and Theoretical Polymer Science* 1988, 8:143-157.
- [17] Kase, S, Matsuo, TJ. Studies of Melt Spinning I. Fundamental Equations on the Dynamics of Melt Spinning, *Journal of Polymer Science Part A* 1965, 3:2541-2554.